Available online at www.sciencedirect.com
SCIENCE DIRECT
Tectonophysics 414 (2006) 169–189
TECTONOPHYSICS
www.elsevier.com/locate/tecto

Paleomagnetic evidence for large en-bloc rotations in the Eastern Alps during Neogene orogeny

Wolfgang Thöny [a,b,*], Hugo Ortner [b], Robert Scholger [a]

[a] Department of Geosciences and Geophysics, University of Leoben, Peter-Tunner-Str. 25, 8700 Leoben, Austria
[b] Institute of Geology and Paleontology, University of Innsbruck, Innrain 52, 6020 Innsbruck, Austria

Received 25 October 2004; received in revised form 9 August 2005; accepted 4 October 2005
Available online 13 December 2005

Abstract

We present new paleomagnetic data from the Northern Calcareous Alps and the Central Alps of Austria. All new data are overprint magnetizations and can be subdivided into two groups: In rocks older than earliest Rupelian, two remagnetizations reflecting both clockwise and counter-clockwise rotation were detected. In rocks of late Rupelian and younger ages, only a counter-clockwise rotated remagnetization was found. Our results together with results from previous paleomagnetic studies from the Eastern and Southern Alps suggest two main phases of vertical axis rotation. The first, clockwise rotation affecting the Northern Calcareous Alps was active between earliest to Late Rupelian. We propose a model where the Northern Calcareous Alps are segmented into individual blocks. Within a dextral shear corridor these blocks rotated clockwise due to the counter-clockwise rotation of the Southern Alps and Central Alps. The second, counter-clockwise rotation occurred in the Late Oligocene to Middle Miocene, affecting Eastern and Southern Alps. In this stage of orogeny, the internal massifs of the Western Alps were already accreted to the upper plate and therefore included in counter-clockwise rotation. This rotation is contemporaneous with counter-clockwise rotation in the Apennines and opening of the Balearic basin, and a genetic relationship is suggested. A second step of counter-clockwise rotation, reconstructed from published data, is observed in the sedimentary basins at the southeastern margin of the Eastern Alps, where counter-clockwise rotated Miocene and Pliocene sedimentary rocks are present. This rotation is seen in connection to a young counter-clockwise rotation of the Adriatic plate.

Keywords: Rotation; Paleomagnetism; Eastern Alps; Adriatic microplate; Shortening; Cenozoic

1. Introduction

The architecture of orogens is mostly discussed in cross-sections perpendicular to the strike of the main thrusts, as the main tectonic units usually have an extremely elongate geometry parallel to the strike of the orogen. Rotational components during convergence are usually neglected because changing directions of shortening through time hinder interpretation and balancing of sections. Nevertheless, rotations are extremely important in orogeny, both on the local and on the orogen scale (Allerton, 1998). This study aims to document the post-Eocene rotational history of the Alpine part of the Adriatic microplate, which is identical to the Austroalpine units of the Eastern Alps together with the Southern Alps (Froitzheim et al., 1996) (Fig. 1).

The Alpine orogenic belt in its present shape is a result of Eocene to Oligocene collision of the Adriatic micro-

* Corresponding author. Department of Geosciences and Geophysics, University of Leoben, Peter-Tunner-Str. 25, 8700 Leoben, Austria.
E-mail address: wolfgang.thoeny@stud.unileoben.ac.at (W. Thöny).

0040-1951/$ - see front matter © 2005 Elsevier B.V. All rights reserved.
doi:10.1016/j.tecto.2005.10.021

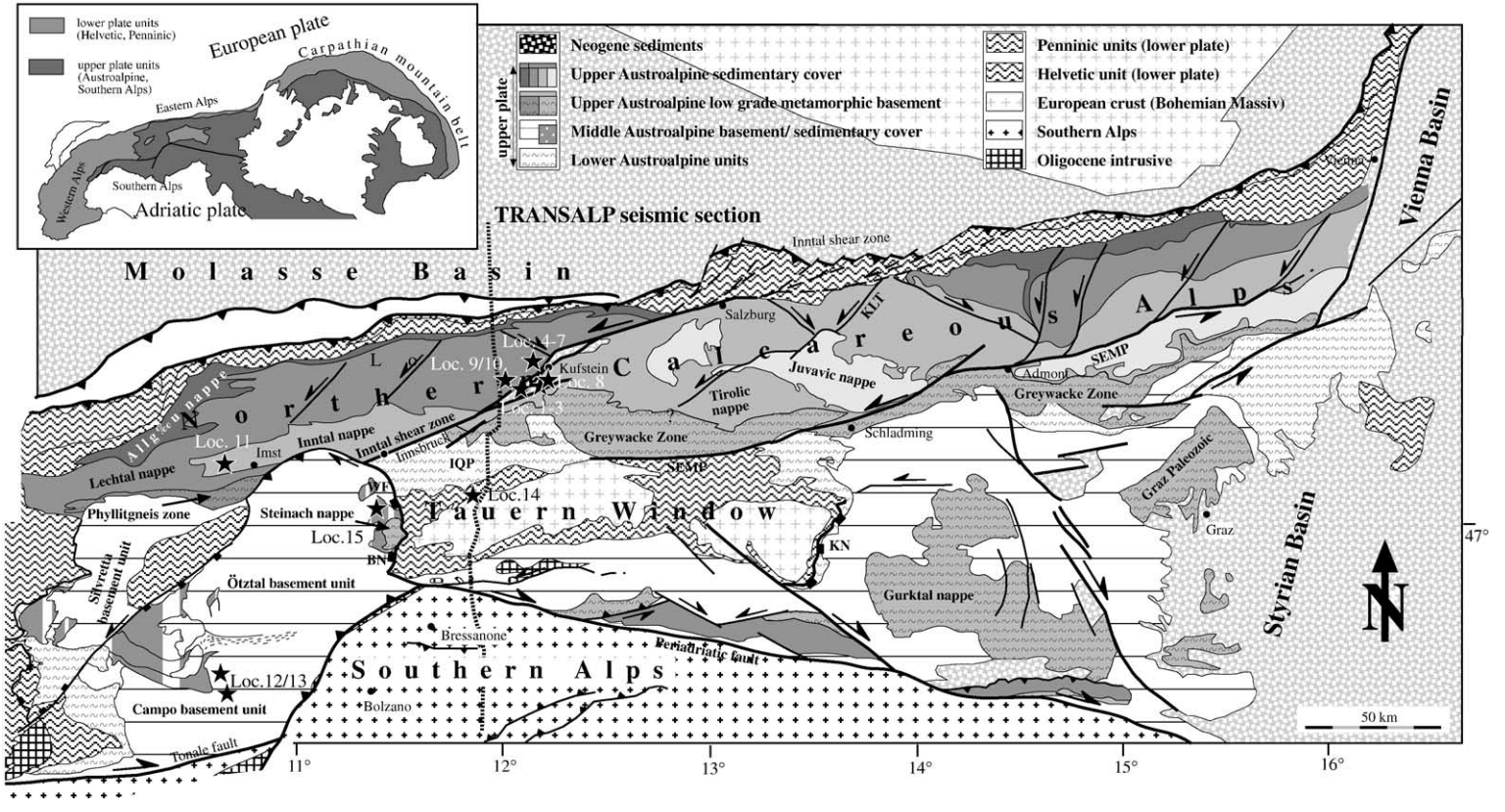

Fig. 1. Geological sketch of the Eastern and Southern Alps with structural units sampled during this study; heavy black lines delineate Cenozoic fault pattern. Inset top left, plate tectonic position of the investigated area in the Alpine arc. Asterisks mark sampling localities.

plate and the subducting European plate. Prior to continental collision the Penninic ocean, which separated the two plates between the Early Jurassic and the Eocene, was subducted below the Adriatic plate. Before Cenozoic orogen, the Adriatic microplate was involved in a Cretaceous orogeny in lower plate position, during which the Meliata–Hallstatt ocean was closed southeast of the present-day Eastern Alps (Froitzheim et al., 1996). Metamorphism in the Austroalpine units is mainly a result of crustal thickening during this so-called Eoalpine event (Thöni and Jagoutz, 1993). The internal structure of the Austroalpine units within the Eastern Alps mainly formed during the Cretaceous (Eoalpine) orogeny (Froitzheim et al., 1994; Neubauer, 1994; Faupl and Tollmann, 1979).

Along the northern margin of the Eastern Alps, the Northern Calcareous Alps form a thin-skinned foreland fold-and-thrust belt built mainly of Mesozoic rocks (Linzer et al., 1995). The thin-skinned units are partly still in contact with their basement units along their southern margin, which are Paleozoic low-grade metamorphic rocks (Greywacke zone). The Northern Calcareous Alps and their basement are tectonically underlain by Paleozoic and older polymetamorphic rocks, which are part of a thick-skinned nappe stack (Innsbruck Quartzphyllite unit; Ötztal, Silvretta and Campo basement units; Fig. 1), which formed during the Eoalpine event. The geometry of the Cretaceous nappe stack did not significantly change during Eocene/Oligocene continental collision, when it moved as a rigid block over tectonically deeper units.

Post-collisional deformation, however, strongly changed the geometry of the nappe stack. The metamorphic core complex of the Tauern window formed by stacking of crustal flakes of the subducting European plate during the Oligocene and Miocene (Lammerer and Weger, 1998; TRANSALP Working Group, 2002). These tectonically deepest units of the Eastern Alps exposed, e.g., in the Tauern window are referred to as Penninic units. Stacking of crustal flakes during the Miocene was combined with major orogen-parallel extension (e.g. Ratschbacher et al., 1991; Lammerer and Weger, 1998). The extension started, when thrusting of the Alpine orogen onto the northern foreland basin stopped (Steininger et al., 1991), so that convergence between the Adriatic and the European plate was compensated by eastward extrusion of crustal blocks (Ratschbacher et al., 1991). Eastward moving crustal blocks were delimited by a system of steep strike-slip faults diverging to the east, which obliquely cut through the Alpine nappe stack (Fig. 1) (Ratschbacher et al., 1991).

We present data from sediments of Late Cretaceous to Oligocene age and data from metamorphic rocks that were affected by Tertiary high temperature metamorphism in the vicinity of the TRANSALP seismic section (TRANSALP Working Group, 2002). The data are interpreted in a larger frame and are, therefore, compared to data from the autochthonous Adriatic plate, the Apennines, the Western Alps and the Alpine foreland basins.

2. Sampling sites

2.1. Northern Calcareous Alps

Inside and south of the Inn valley fault system Oligocene sediments were sampled at 3 localities (Fig. 1, Table 1). Upper Rupelian turbiditic silt/sandstones were sampled in Unterangerberg (locality 1). Locality 2 (Häring) comprises two sites with Lower to Upper Rupelian marls belonging to the Paisslberg Formation (Ortner and Stingl, 2001). Carbonates of the Lower Rupelian Werlberg Member (Ortner and Stingl, 2001) were sampled at locality 3 (Bruckhäusl).

Upper Cretaceous carbonates and marls as well as Eocene turbidites were sampled in Lechtal and Inntal nappes (Fig. 1, Table 1). The stratigraphic age of these sites (localities 5–11) ranges from Early Santonian to Middle Eocene. Arenites at locality 4 (Gfallermühle) belong to the Upper Eocene Oberaudorf Formation, which exhibits a prominent erosive discordance from the Gosau Group (Ortner and Stingl, 2001).

At locality 5 (Sebi) Middle Eocene turbidites (Hagn, 1982) and nearby Maastrichtian carbonates (Jung et al., 1978) are exposed (locality 6). Campanian silt/sandstones (Risch, 1985) could be sampled at locality 7 near Hechtsee, and Upper Campanian marls (Gruber, 1997) at locality 8 (Schwoich). Upper Santonian marls (Sanders, 1998) were sampled in 4 sites at Mühlbach (locality 9) and Lower Santonian marls in two sites at Mösl (locality 10). Locality 11 (Muttekopf) is characterized by a northward tilted syncline with a fold axis trending NE/SW (fold axis 71/25). The final stage of folding is not reached before Tertiary (Ortner, 2001). From both limbs of this syncline, 6 sites were chosen in mainly neritic to deep marine Santonian marls.

2.2. Central Alps

Oligocene dykes were sampled in 5 sites at two localities in the Campo nappe of the Central Alps (Fig. 1, Table 1). The dykes outcropping at localities 12 and 13 (Hintergrat and Gran Zebru') were related to the contemporary Oligocene Gran Zebru pluton. The

Table 1
Basic geographical and geological data of the paleomagnetic sampling localities

Locality no.	Locality	Dec (in situ)	Inc (in situ)	α_{95}	K	Dec (abc)	Inc (abc)	α_{95}	K	N	Lith. age	Dip	Site abbrev.	Latitude	Longitude	Lithology
Northern Calcareous Alps																
1	Unterangerb.	306	56	8.7	23.9	255	22	10.5	13.5	13	E.Oligocene	mean	UA	47,499	12,058	Siltstone
2	Häring	307	54	9.5	18.3	308	15	9.7	17.7	14	E.Oligocene	310 / 40	ZM	47,501	12,124	Marls
3	Bruckhäusl	60	46	5.6	142.5	76	86	6.7	101.4	6	Rupelian	236 / 40	BH	47,495	12,101	Carbonates
4	Gfallermühle	40	61	17.4	8.7	2	67	neg FT	2.7	10	Priabonian	mean	GF	47,634	12,166	Carbonates
5	Sebi	22	41	14.7	13.3	15	68	27.1	4.6	9	M. Eocene	mean	SB	47,648	12,236	Marls
6	Sebi	27	53	15.6	19.3	287	85	16.9	16.6	6	Maastricht.	220 / 39	SBM	47,649	12,235	Carbonates
7	Hechtsee	17	56	14.6	28.2	170	78	14.7	28.1	5	Campanian	190 / 45	IHG	47,612	12,171	Siltstone
8	Schwoich	326	51	10.2	17.4	323	30	12.7	11.6	13	L.Campanian	320 / 20	SZM/NS	47,542	12,164	Marls
9	Mühlbach	334	48	9.9	24.5	273	67	11.3	19.2	10	L.Santonian	175 / 36	NF	47,501	11,915	Marls
	Mühlbach	12	15	8.9	27	19	49	8.9	27	11		175 / 36	NF			
10	Mösl	339	57	9.7	33.6	291	77	8.5	43.4	8	E.Santonian	190 / 40	IMG	47,503	11,897	Marls
	Mösl	18	9	9.1	72.3	20	48	9.1	72.1	5		190 / 40	IMG			
11	Muttekopf	307	49	10.9	31.5	116	69	34.5	4	7	Santonian	mean	MG	47,251	10,592	Marls
	Muttekopf	209	−47	15	27.1	200	32		2.2	5		343 / 77	MG3			
	Muttekopf	52	49	9.6	26.5	89	26	13.4	13.9	10		137 / 48	MG4+MG7			
	Muttekopf	44	49	8.1	23.1	108	36	neg.FT	2.7	15		mean	MG			
Central Alps																
12	Hintergrat	335	56	3.2	67					30	E.Oligocene		HG	46,502	10,577	Basaltic dyke
13	Gran Cebru	316	60	9.9	24.6					10	E.Oligocene		AZ/IZ	46,486	10,589	Basaltic dyke
14	Hochstegen	334	63	6.9	37.1					13	Malmian		HST	47,157	11,844	Marble
	Hochstegen	43	57	10.6	28.1					10	Malmian		HST			
15	Serles	319	14	7.7	75.9	318	39	7.8	74.5	6	Permoskyth.	144 / 25	BS	47,124	11,361	Sandstone

Locality no. refers to numbers in Fig. 8. Paleomagnetic results concerning Eocene/Oligocene remagnetization and prefolding magnetizations. Dec/Inc in situ=declination/inclination before any correction, Dec/Inc (abc)= declination/inclination after bedding correction, K=precision parameter; α_{95}=radius of cone of 95% confidence about the mean direction (Fisher, 1953), N=number of samples used to calculate the mean, Age=Lithology age, Dip=dip direction/dip.

magmatism is dated to the Late Rupelian (Dal Piaz et al., 1988).

For comparison, marbles of the Helvetic Hochstegenzone were sampled (locality 14) at the northern rim of the Tauern Window (Lammerer, 1986; Thiele, 1976), as well as Permoskythian sediments at Serles/Margarethenbach (locality 15) in the parautochtonous sedimentary cover of the Oetztal/Stubai basement complex (Stingl and Krois, 1990; Krois et al., 1990) (Fig. 1, Table 1).

3. Methods

The paleomagnetic samples were collected with a water cooled coring apparatus and oriented with a magnetic compass. Natural remanent magnetization was measured on a three-axis cryogenic magnetometer complete with an in-line degausser (2G Enterprises). Specimens were subjected to detailed stepwise demagnetization procedure (alternating field and/or thermal treatment). During thermal demagnetization, the bulk susceptibility of the specimens was routinely measured to observe possible mineral transformations (Collinson, 1983).

Isothermal remanent magnetization (IRM) acquisition and backfield experiments aimed at the identification of the magnetic mineral content of a representative number of pilot specimens (Lowrie, 1990). A three component IRM was induced at 2.5 T, 0.5 and 0.1 T and thermally demagnetised afterwards. Geofyzika KLY-2 and Digico instruments were used for measuring magnetic susceptibility and anisotropy of the magnetic susceptibility (AMS). The latter (Tarling and Hrouda, 1993) aimed at determining the origin of the magnetic fabric with respect to the sedimentary bedding planes.

Paleomagnetic data analysis included principal component analysis (Kirschvink, 1980) based on visual inspection of orthogonal projections (Zijderveld, 1967). Mean directions were calculated using TectonicsFP (Ortner et al., 2002). Fold tests after McElhinny (1964) were carried out with the help of SuperIAPD program by Torsvik et al. (1996). All measurements were carried out in the Paleomagnetic Laboratory of the University of Leoben.

4. Results

4.1. Northern Calcareous Alps

4.1.1. Oligocene sediments

The remanent magnetization of the Rupelian siltstones and marls at localities 1 and 2 was dominated by a magnetite-like phase, which could be identified through acquisition of isothermal remanent magnetization (Fig. 2) and demagnetization paths towards the origin during alternating field demagnetization in the range between 5 and 15 mT (Fig. 2). The corresponding unblocking temperatures were observed during thermal demagnetization around 350 °C. Both sites yielded well grouped magnetization components with NW directed declinations before bedding correction (Fig. 2, Table 1), indicating counter-clockwise rotation after remagnetization. A statistically significant negative fold test (C_r=1.98 according to McElhinny, 1964) indicated that the overprint took place after folding. The time of remagnetization and rotation is therefore younger than the age of folding of the Rupelian sediments.

Lower Rupelian carbonates from locality 3 are characterized by demagnetization paths towards the origin in the range from 200 to 500 °C, or between 15 and 80 mT. Magnetite was the main carrier of the remanent magnetization, but minor contributions from pyrrhotite were observed in some samples. The mean paleomagnetic direction for this group shows a north-easterly declination before bedding correction (Table 1). Measurements of anisotropy of magnetic susceptibility yielded disturbed magnetic fabric for all samples from locality 2 (Häring). The degree of anisotropy is low (3.1–4.8%), the fabric is typically foliated.

4.1.2. Upper Cretaceous/Eocene sedimentary rocks

Samples from Eocene and Upper Cretaceous sedimentary rocks at localities 4 to 7 showed successful demagnetization with the alternating field method. Well grouped demagnetization vectors, which typically deflected from the origin, were observed in the range between 5 and 30 mT (Fig. 3A, Table 1). Thermal demagnetization in the temperature range up to 500 °C was successful as well. IRM acquisition curves clearly identified magnetite to be the main carrier mineral. We observed scattered paleomagnetic vectors with north-easterly declinations.

The two Eocene localities (4 and 5) yielded statistically significant negative fold tests (Table 1). Mc Elhinny tests indicated best *k*-values at 20% unfolding (C_r=2.22 and 2.33 for localities 4 and 5, respectively). The observed clockwise rotation occurred subsequent to the remanence acquisition, which took place in a late stage of folding.

Two sub-parallel components of magnetization could be isolated in marls of Campanian age from locality 8, Schwoich. Thermal demagnetization yielded unblocking temperature spectra of 100–300 and 400–500 °C (Fig. 3B, Table 1). Accordingly, the same components could be discriminated by applying alternating fields in the ranges between 2–20 and 30–50 mT. Also IRM

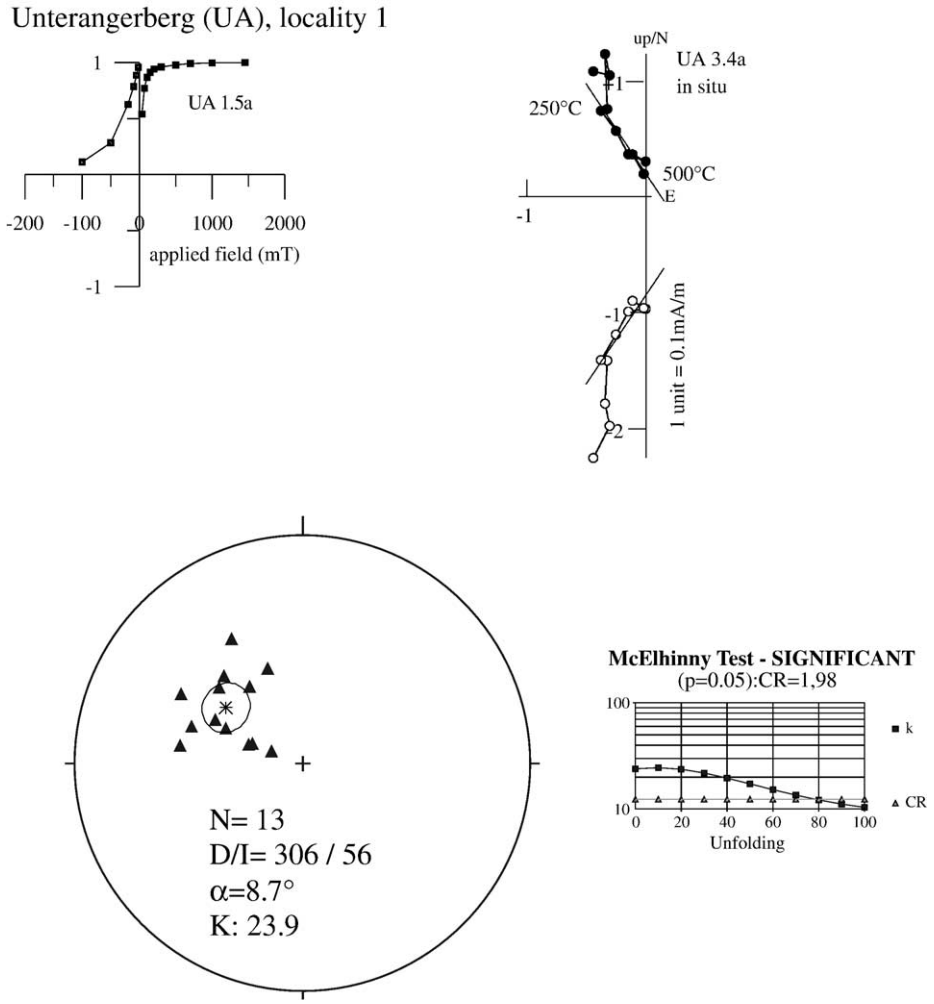

Fig. 2. Rock magnetic properties, demagnetization behavior and statistical parameters from localities 1–3. Typical IRM acquisition curve (Lowrie, 1990). Zijderveld demagnetograms of representative samples in geographic coordinates. In the Zijderveld diagrams, full/hollow circles: projection of the NRM in the horizontal/vertical plane. Stereographic projection of the characteristic remanence magnetization direction, in situ coordinates; significant negative fold tests (McElhinny, 1964).

acquisition curves indicated two different magnetic minerals, a low-coercive mineral (most probably magnetite) and a high coercive mineral such as pyrrhotite. Each of these minerals was carrying about 50% of the observed natural remanent magnetization, but no significant differences in the directions could be observed. The mean paleomagnetic direction before bedding correction (Table 1) derived from well grouped vectors representing both polarities gave evidence for counterclockwise rotation (Dec=326; Inc=51).

Due to very similar bedding planes there was no significant proof for the timing of the remanence acquisition with respect to the tectonic tilting from a fold-test. However, the observed larger scatter of the vectors after bedding correction gave evidence for post-tilting remagnetization and subsequent counterclockwise rotation.

Marls of Santonian age (localities 9–10) yielded well defined demagnetization paths towards the origin during thermal demagnetization. Two different components of magnetization were observed (Fig. 3C, Table 1). The lower temperature component unblocked at temperatures below 400–450 °C and was characterized by NW-directed declinations with positive inclinations before bedding correction. The second component was isolated up to 560–580 °C and showed NNE-directed declinations before bedding correction. Samples from one site in red marly mudstone at locality 9 showed a significant contribution from hematite in the IRM-curves (Fig. 3B), although the main carrier of the

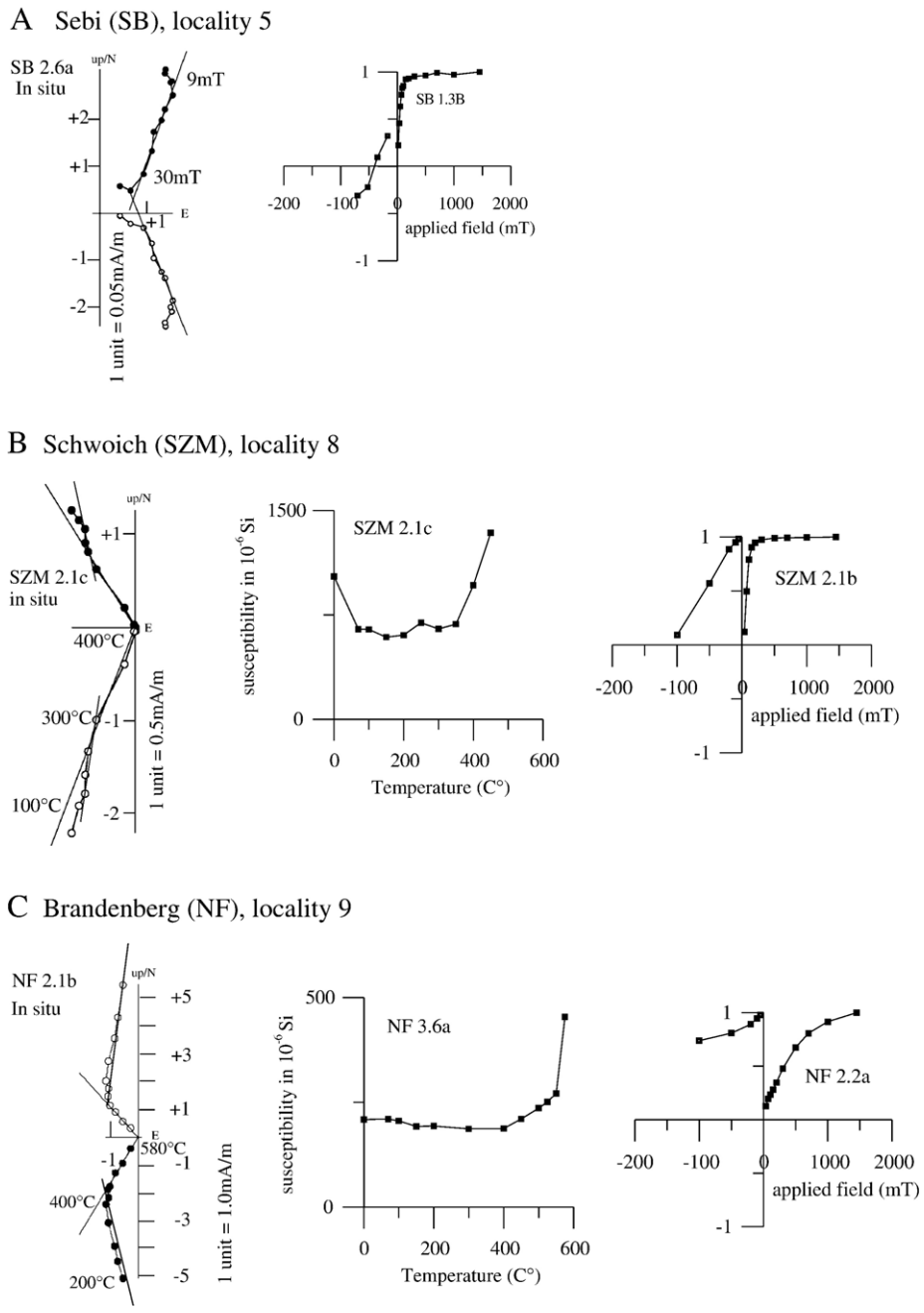

Fig. 3. Rock magnetic properties, demagnetization behavior and statistical parameters from localities 4–11. Typical IRM acquisition curves (Lowrie, 1990). Zijderveld demagnetograms of representative samples in geographic coordinates, and susceptibility versus temperature curves. In the Zijderveld diagrams, full/hollow circles: projection of the NRM in the horizontal/vertical plane.

natural remanent magnetization was magnetite. The shallow inclinations of the mean paleomagnetic directions before bedding correction could be explained with a synfolding origin of the remagnetization vectors.

At locality 11 (Muttekopf), two components of magnetization with different directions were observed, which resided in the same magnetic mineral with unblocking temperatures up to 500 °C (Fig. 3C). Alternating field demagnetization was successful in the range between 3 and 30 mT (Fig. 3C). IRM acquisition curves indicated magnetite as main magnetic carrier mineral. The declinations of the two components were

NW- and NE-directed (Fig. 3C; Table 1). Both components yielded negative fold tests with the maximum *k*-value (according to McElhinny, 1964) at 0% unfolding: C_r=1.89 for the NE-component; C_r=2.69 for the NW-component (Fig. 4).

Measurements of anisotropy of magnetic susceptibility typically yielded sedimentary, foliated fabrics with a varying degree of anisotropy that is mostly below 5%. The differences were interpreted to result from the deposition by turbidity currents, due to variable current velocities at different times. Disturbed magnetic fabrics were only observed in the Campanian silt-/sandstones at locality 7 (Hechtsee) with K_{min}- and K_{int}-axis tilted to the north and K_{max}-axis aligned WSW within the bedding plane, and in the Santonian marls at locality 11 (Muttekopf). There was no evidence for a

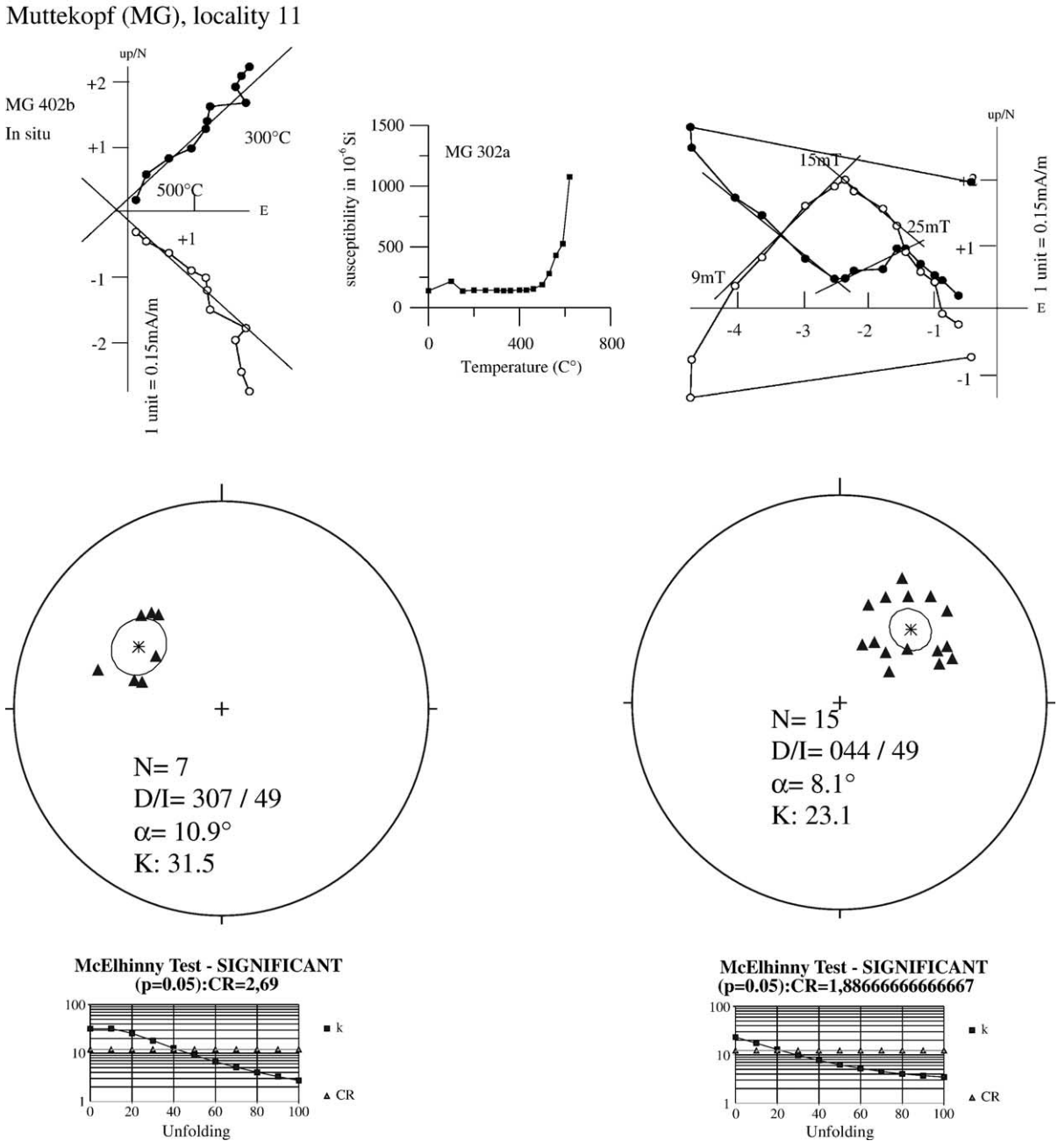

Fig. 4. Stereogeographic projection of the characteristic remanence magnetization direction, in situ coordinates; significant negative fold tests (McElhinny, 1964).

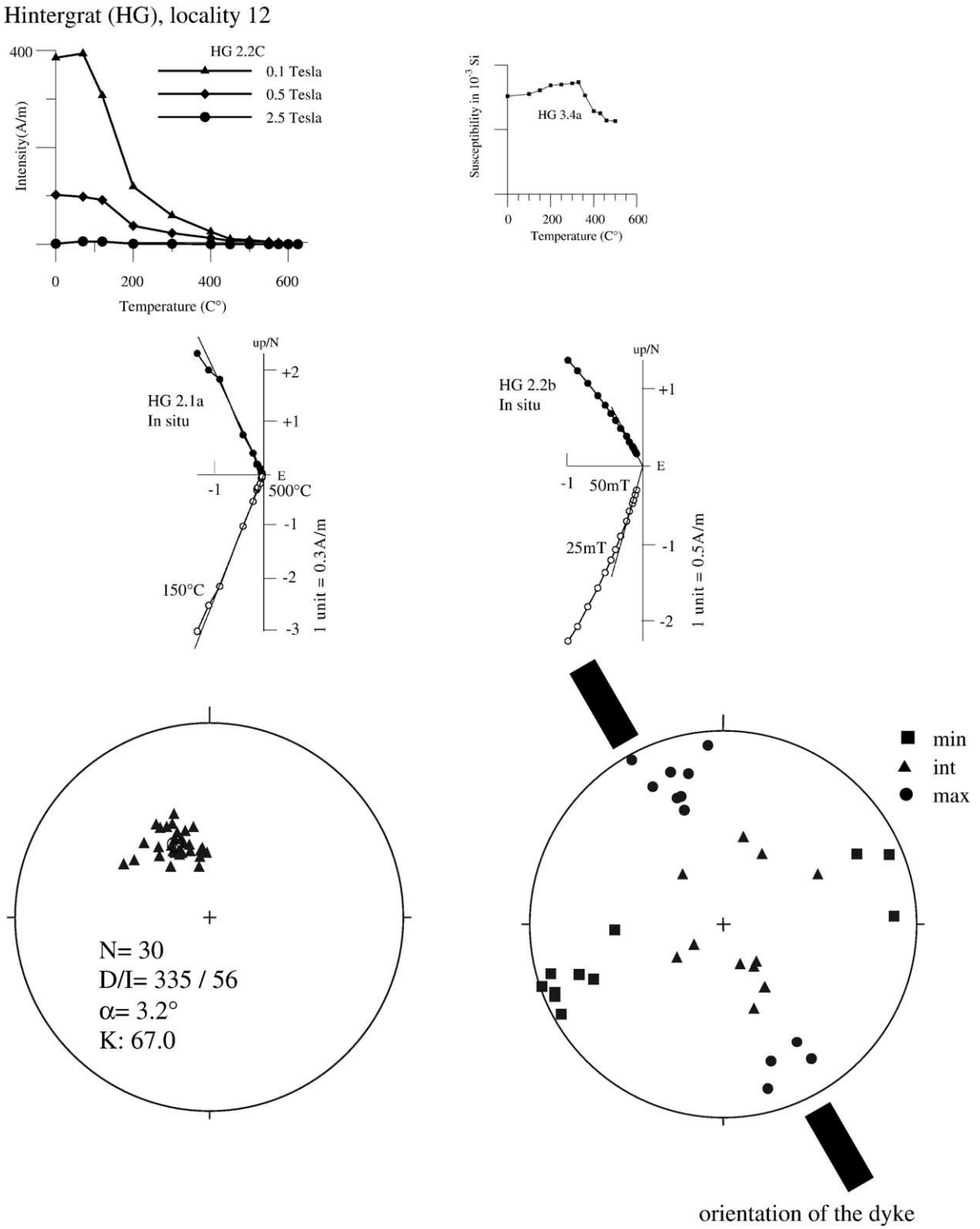

Fig. 5. Rock magnetic properties, demagnetization behavior and statistical parameters from localities 12–15. Typical IRM acquisition curves and thermal demagnetization of three component IRM (Lowrie, 1990). Zijderveld demagnetograms of representative samples in geographic coordinates, and susceptibility versus temperature curves. In the Zijderveld diagrams, full/hollow circles: projection of the NRM in the horizontal/vertical plane.

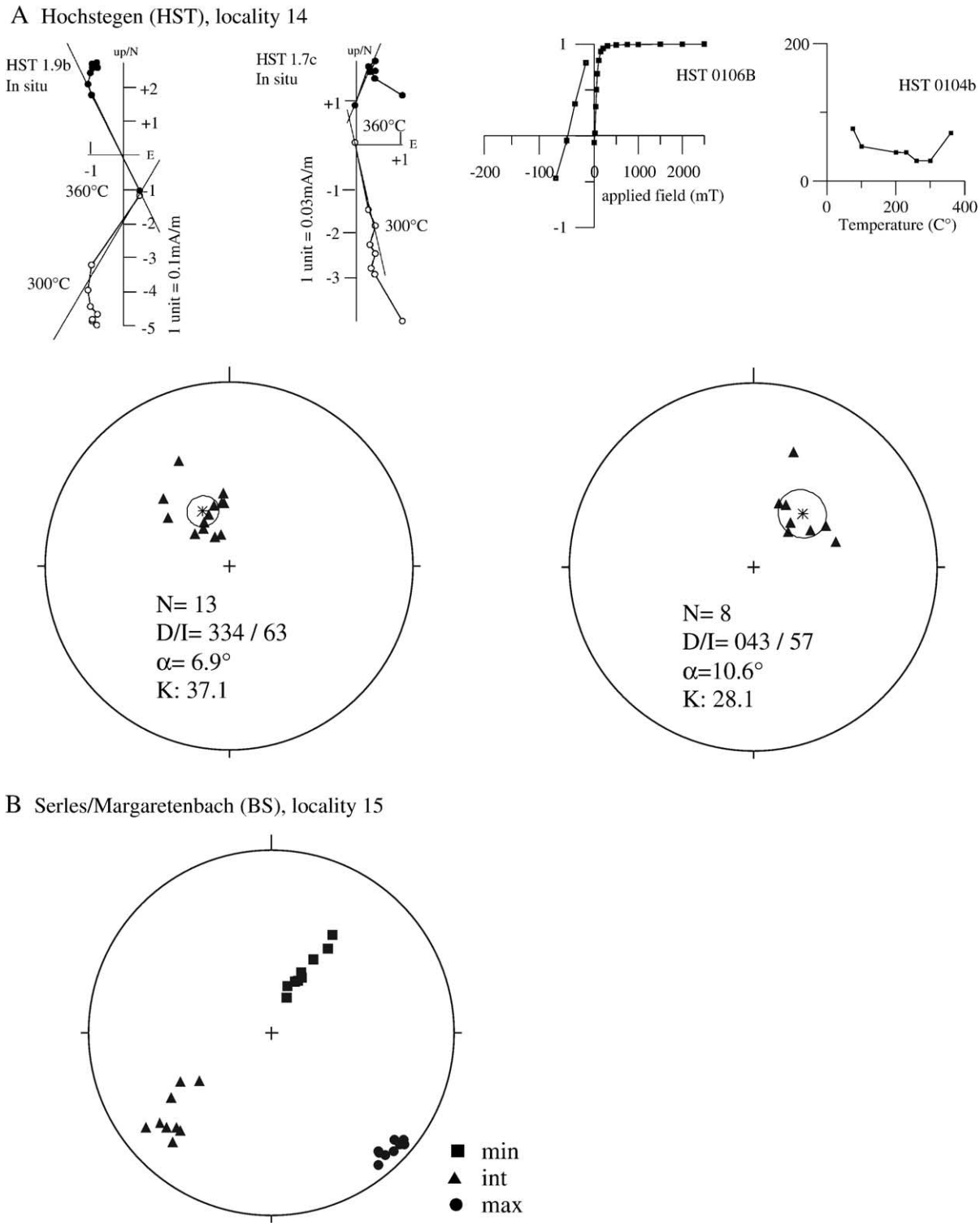

Fig. 6. Stereogeographic projection of the characteristic remanence magnetization direction, insitu coordinates; and AMS results for sites from the Central Alps, in situ coordinates.

correlation between the distribution of the paleomagnetic vector components and the magnetic fabric.

4.2. Central Alps

4.2.1. Oligocene dykes

After removal of a viscous magnetization component at the beginning, all samples from localities 12 and 13 yielded one-component demagnetization paths towards the origin. The component could be thermally demagnetized in the temperature range between 460 and 550 °C, and with alternating fields between 3–50 mT (Fig. 5A). Three-component IRM experiments were identifying a system of low to medium coercive minerals (Fig. 5A). Due to the relatively high alternating fields that were needed to demagnetize the ChRM and varying unblocking temperatures, titanomagnetite with different titanium content was supposed to be the main magnetic carrier mineral. However, the susceptibility decrease between 250 and 500° C on heating gives evidence for maghemite in the samples (Fig. 5).

Well grouped vector components gave mean paleomagnetic directions before bedding correction (Dec=335; Inc=56 and Dec=316; Inc=60) for localities 12 (Fig. 5) and 13, with evidence for counter-clockwise rotation after cooling below Curie temperatures or subsequent remagnetization.

All samples showed similar magnetic fabrics, with subhorizontal K_{max}- and nearly vertical K_{int}-axes in alignment with the orientation of the dyke (Fig. 5), except for a single site where the magnetization vectors were aligned with the K_{min}-axes. All other sites showed no dependence from the magnetic fabric. The degree of anisotropy is low (0.9–4.7%), the fabrics are foliated.

4.2.2. Metamorphic rocks

Thermal demagnetization of marbles from locality 14, Hochstegen, yield very low unblocking temperatures in the range between 250–360 °C (Fig. 6A). During isothermal remanent magnetization experiments, the samples rapidly acquired saturation at field strengths below 100 mT, but the backfield curves show a relatively high remanence coercivity (Fig. 6A). According to Maher and Thompson (1999) IRM(1 T)/χ ratio is indicating MD (multi-domain) titanomagnetite, maghemite or magnetite as carrier minerals. From these observations, especially due to the very low unblocking temperatures, titanomagnetite was supposed as carrier mineral of magnetization. The decrease of the susceptibility during heating cannot be explained by now.

Analyses of the demagnetization paths yielded two groups of magnetization components, which differed in the orientation but are carried by the same mineral. The components were directed NW and NE, both with positive inclination values before bedding correction (Fig. 6B, Table 1). Most of the samples showed negative susceptibilities. Therefore a magnetic fabric could not be calculated.

Samples of Permoskythian sandstones from locality 15 (Serles/Margarethenbach) could be successfully demagnetized with temperatures ranging up to 500 °C and with alternating field strengths between 3 and 30 mT. Susceptibility did not change during heating up to 600 °C. Well grouped vectors gave a mean direction with a declination of 320° and an inclination of 14° before bedding correction (Table 1). The shallow inclination of this overprint magnetization may be explained by southward tilting of the Ötztal–Stubai basement nappe during northward directed thrust movement upon the Northern Calcareous Alps during a very young process.

All samples showed similar magnetic fabrics, with a subvertical orientation of K_{min} and subhorizontal, SW and SE directed orientation of K_{int} and K_{max} (Fig. 6B). The degree of anisotropy is between 26% and 38.8%. The degree of lineation and foliation is between 10.9% and 20.9%. The magnetic vectors showed no dependence from the magnetic fabric.

5. Discussion and conclusions

5.1. Mechanism and age of remagnetization

The hypotheses presented in this paper rely on the interpretation that all observed magnetizations represent magnetic overprints acquired after tectonic deformation. The interpretation as secondary magnetizations is based on negative fold tests (McElhinny, 1964). As the Northern Calcareous Alps were not affected by metamorphism, except in their southernmost part, increased fluid flow causing diagenetic alteration of carbonates is most probably the reason for chemical remagnetization, even if this alteration is not easy to see in thin section. Magnetic particles are extremely small and can be mobilized or grow also when the amount of fluid passing the rocks is small (Suk et al., 1993). In regional studies of carbonate cements from the Eastern Alps, Zeeh et al. (1997) and Kappler and Zeeh (2000) concluded that five of six generations of cements occurring in carbonates are of Cenozoic age, most of them even of post-Oligocene age. Ortner (2003) described intense local cementation of Oligo-

cene age. This gives evidence for intense fluid flow during continental collision and post-collisional deformation in the Eastern Alps, which most probably caused chemical remanent remagnetization.

Some of the magnetization directions found in the Northern Calcareous Alps with NE-trending declinations are close to the magnetization values for stable Europe at 10–5 Ma (Besse and Courtillot, 2002). Consequently, an unrotated overprint magnetization of Late Miocene age might also cause these directions. Thus, no components carried by goethite were included into mean value calculations as goethite is the main carrier mineral of the (sub)recent earth magnetic field.

Two events of remagnetization differing in the declination directions can be distinguished in the working area. In the area of the Inn valley in the Northern Calcareous Alps, where a more or less complete Cretaceous to Oligocene sedimentary succession is preserved, remagnetizations with clockwise rotated declinations are found in rocks of Early Rupelian and older age (Fig. 7). Remagnetizations with counter-clockwise rotated declinations were observed in the entire sedimentary succession.

In metamorphic marbles of the Penninic zone (site HST, locality 14) at the northern margin of the Tauern window (Fig. 8), we isolated two components of remagnetization, with clockwise and counter-clockwise rotated declinations, respectively. Both overprints were blocked below temperatures between 300 and 360 °C, as the carrier mineral of magnetization is titanomagnetite. ^{40}Ar–^{39}Ar data from white mica from samples in the same structural position east of our site HST (locality 14) gave formation ages of 28–35 Ma (Urbanek et al., 2001). This gives an maximum age estimate for both remagnetizations observed, as the ^{40}Ar–^{39}Ar system for white mica closes between 325 and 375 °C. In the Central Alps magnetization directions were derived from Oligocene dykes in the Ortler Mountains, which show a counter-clockwise rotated declination. These dykes are interpreted to be part of the dyke swarms related to the Gran Zebrú pluton (Mair and Purtscheller, 1995), which is dated radiometrically to the Late Rupelian, 32 Ma (Dal Piaz et al., 1988).

The oldest rock, which is just affected by one, i.e. the counter-clockwise rotated remagnetization, is Late Rupelian in age. Because clockwise rotation must postdate the age of the youngest rocks, which show a clockwise rotated remagnetization (i.e. earliest Rupelian) and must predate the second, counter-clockwise rotated remagnetization, the Northern Calcareous Alps data set (locations 1–11; Fig. 7) suggests that clockwise rotation was active between earliest and Late Rupelian times.

The youngest rocks sampled in the Northern Calcareous Alps are of Late Rupelian age (locations 1, 2) and are only affected by a 30° counter-clockwise rotated remagnetization. Therefore the data presented in this paper establish a post-Rupelian age for counter-clockwise rotation. The age of remagnetizations in the Central Alps (locations 12–15) is less well constrained, but do not contradict remagnetization ages in the Northern Calcareous Alps. In all cases, remagnetization ages postdate the Eocene/Oligocene boundary (see above).

5.2. Clockwise rotation

Reliable data indicating Cenozoic clockwise rotation of the Northern Calcareous Alps and their basement were presented previously (Pueyo et al., 2002; Schätz et al., 2002), additional data are presented in this study. Schätz et al. (2002) already suggested that many of the "primary" paleomagnetic data from the Northern Calcareous Alps with clockwise rotated declinations (e.g. Hargraves and Fisher, 1959; Mauritsch and Becke, 1987; Channell et al., 1990, 1992) are in fact secondary magnetizations. We follow this interpretation. South of the Northern Calcareous Alps, Cenozoic clockwise rotation is poorly documented (HST, location 14). According to our data the clockwise rotation was active between earliest and Late Rupelian times. A working hypothesis for the Cenozoic clockwise rotation of the Northern Calcareous Alps independently of the Central Alps proposes clockwise rotation of segments of the Northern Calcareous Alps between ENE- to NE-trending sinistral faults in a domino style (Fig. 9). The process was possibly driven by young anticlockwise rotation of Adria and the Central Alps in respect to Europe (e.g., Besse and Courtillot, 2002), leading to the formation of a mega-shear zone ("dextral wrench corridor") in the area of the Northern Calcareous Alps between the Central Alps and the European Foreland.

Two problems regarding this interpretation have to be kept in mind: The amount of clockwise rotation is 60°, which is the difference between the mean of the clockwise rotated magnetizations and the mean of the counter-clockwise rotated magnetizations. Such large rotations within the dextral wrench corridor would only be possible if using a "soft domino model" instead of a "rigid domino model" (Peacock et al., 1998) due to major space problems: 60° rigid block rotation of blocks with a height to width ratio of 1 : 1.5 would cause elongation of 100% parallel to the wrench corridor. Large gaps would open at the edges of the rotating blocks. Therefore the blocks must be allowed to deform internally, and we should expect inhomogeneous clockwise rotation. Neither the

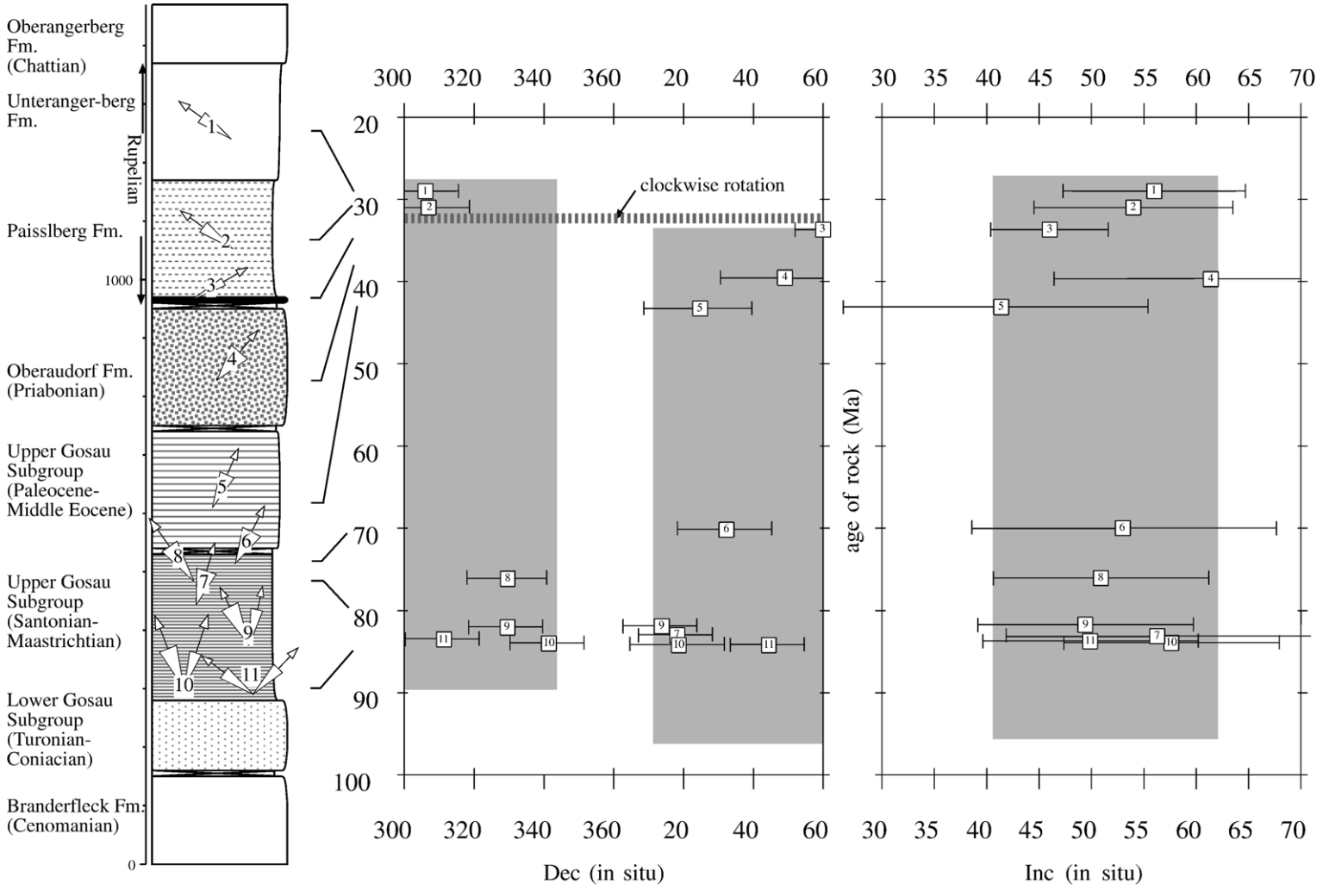

Fig. 7. Stratigraphic summary section of Late Cretaceous to Oligocene rocks in the Unterinntal area and associated cross plots of age of rock and declination/inclination of secondary magnetizations. Note that declinations do not change systematically with age of rock. Shaded squares illustrate mean direction of inclinations and declinations of clockwise and counter-clockwise rotated magnetizations in the Unterinntal area in Cenozoic times. Numbers at arrows refer to Table 1.

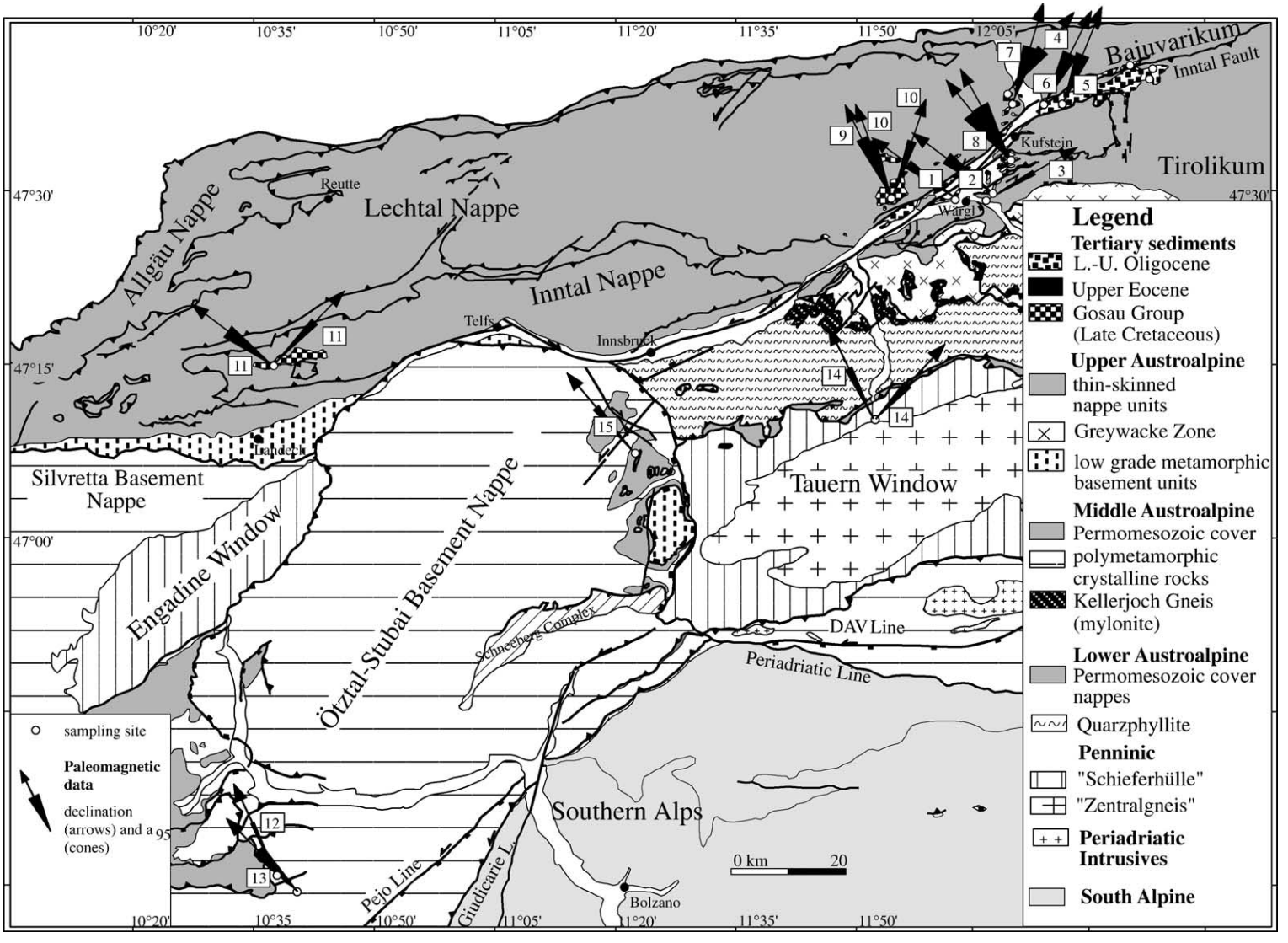

Fig. 8. Geological sketch of the study area comprising the western part of the Eastern Alps and the northern part of the Southern Alps. Arrows indicate trend of declinations, and cones depict α_{95}. Numbers at arrows refer to Table 1.

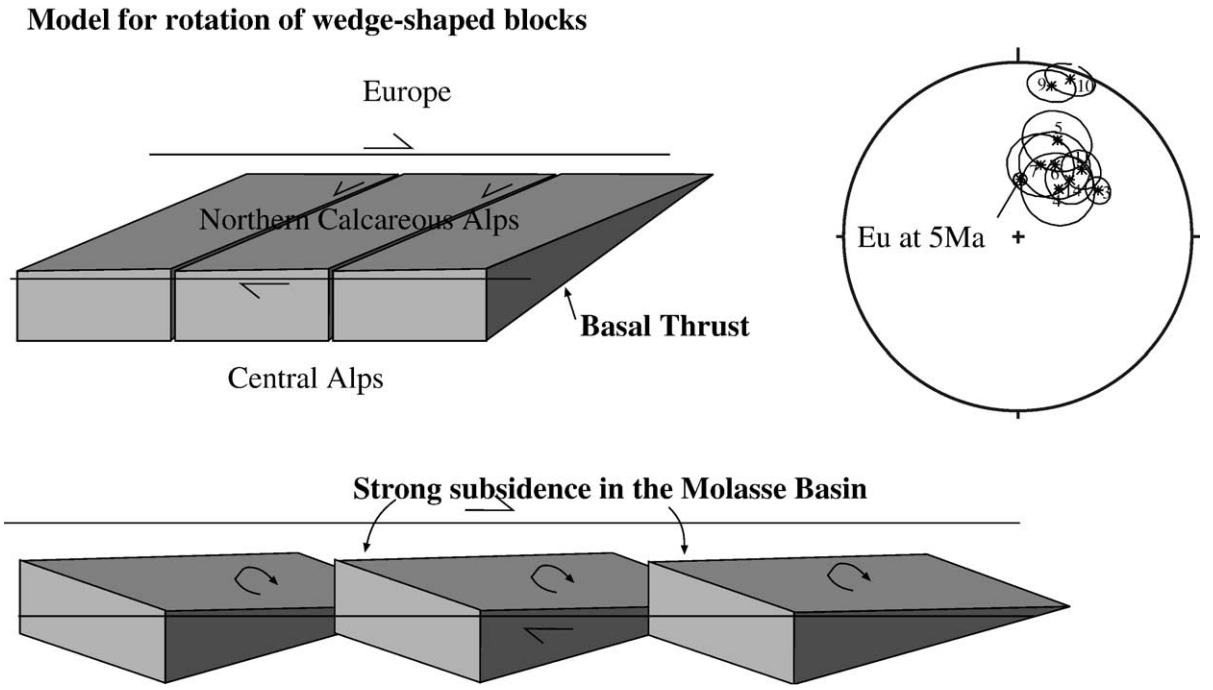

Fig. 9. Model for clockwise rotation in the Northern Calcareous Alps. Data (lower hemisphere plot, Table 1, Fig. 8) indicate homogeneous rotation values.

gaps, i.e. sedimentary basins, are observed nor is the space available for 100% elongation, and clockwise rotation is rather homogeneous (Fig. 9).

Secondly, finite counter-clockwise rotation of the units south of the Northern Calcareous Alps should be larger than counter-clockwise rotation within the Northern Calcareous Alps, because, according to the model presented above, these units should rotate counter-clockwise, while the latter rotated clockwise. According to the data presented in this study, all units were subject to a uniform counter-clockwise rotation (Fig. 10). Therefore we speculate that the Northern Calcareous Alps and the units to the south rotated clockwise uniformly, in spite of scarce direct evidence of clockwise rotation in the latter units (location 14).

5.3. Counter-clockwise rotation

In the following paragraphs, Cenozoic counter-clockwise rotations are discussed in the frame of previously published data from the Alps. Counter-clockwise rotated declinations in overprint magnetizations in the western Northern Calcareous Alps were observed only locally in previous studies (Channell et al., 1992), however this study adds a larger dataset from Oligocene and older rocks (see above). Primary paleomagnetic data from Karpatian/Badenian sedimentary rocks from the eastern part of the Alpine foreland basin (Scholger and Stingl, 2002). Data from intra-Alpine Middle Miocene sedimentary basins (Márton et al., 2000) indicate two stages of counter-clockwise rotations. 30° of counter-clockwise rotation is related to the lateral escape in Ottnangian to Karpatian. Another 30° counter-clockwise rotation is explained by "en block" rotation of the Eastern Alps in Late Karpatian to Pannonian times. According to the published data available, aided by geological arguments, we subdivide the counter-clockwise rotation into two steps.

5.3.1. Late Oligocene to Middle Miocene counter-clockwise rotation

Counter-clockwise rotated declinations in Cenozoic rocks were not only reported in this study (see Fig. 10 and Table 2 for a compilation). In the wider vicinity outside the Eastern Alps, Márton et al. (2003a,b,c), Thio (1988), Vandenberg (1979) and Bormioli and Lanza (1995) reported counter-clockwise rotations from the Southern Alps and their foreland. Also the internal massifs of the Western Alps (Thomas et al., 1999; Collombet et al., 2002) and the Sesia–Lanzo zone (Lanza, 1977, 1978) were affected by Late Oligocene to Middle Miocene counter-clockwise rotation. The external massifs are not rotated with respect to the European plate (Heller, 1980; Crouzet et al., 1996; Aubourg

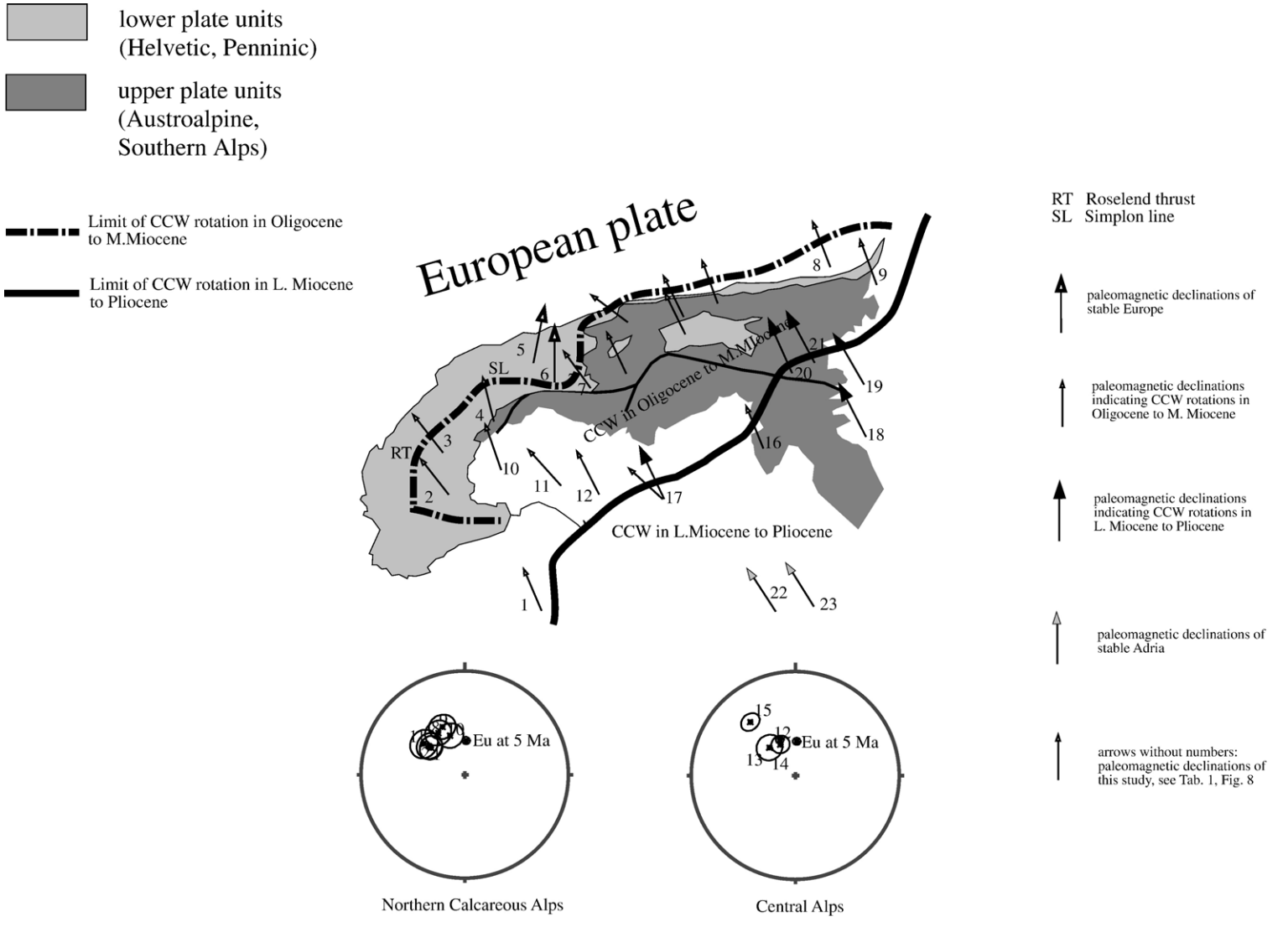

Fig. 10. Tectonic units of the Alps affected by Late Oligocene to Middle Miocene counter-clockwise rotation. Lines are indicating limits of counter-clockwise rotated areas at distinct times. RT = Roselend thrust, SL = Simplon line. Arrows show paleomagnetic results from literature indicating counter-clockwise rotation. Numbers at arrows refer to Table 2.

Table 2
Selected Tertiary and Cretaceous results from Western and Eastern Alps, the Apennines and stable Adria

Locality no.	Locality	Age of ChRM	*N*	Dec of ChRM	Inc of ChRM	*K*	α_{95}	Reference
Stable Adria								
23	Gargano	Turon–Senon	21sites	328	38	21	4	Vandenberg (1983)
22	Murge	Cenom.–Senon	12 sites	327	40	42	7	Márton and Nardi (1994)
12	Voltri, Liguria	L. Eoc.–E. Oligo.	33 samples	333.2	50.3		5.8	Vandenberg (1979)
11	Ramero–Garb.	L. Oligo.–E.Mioc.	10 sites	318	38	62.3	5.5	Hong Kie (1988)
10	Turin mountains	Mid E. Miocene	51 samples	340.8	46.7		9	Bormioli and Lanza (1995)
16	Istria	E.–L. Cretac.	3 localities	318	44	56	17	Marton and Veljovic (1983)
16	Istria	Senon	3 sites/19 sampl.	341	56	150.5	10.1	Marton and Veljovic (1983)
16	Istria	Eocene	8 sites	340	49	30	10	Márton et al. (2003a,b,c)
Pannonian Basin								
19	Mura zala	Karptian–Pontian	8 sites	326	62	50.5	7.9	Marton et al. (2002a)
18	North. Croatia	Pontian	22 samples	333	66	160	10	Marton et al. (2002b)
Western Alps								
3	Brianconnais	Oligocene	9 sites	142.3	−57	44	8	Thomas et al. (1999)
2	Ubaye	Oligocene	12 sites	121	−52	17	11	Collombet et al. (2002)
4	Sesia lanzo	L. Oligocene	5 sites	157.2	−39.3		9.7	Lanza (1977)
5	Aar massif	Oligocene	21 samples	6.7	70.1		8.1	Heller (1980)
			6 samples	15.3	74.2		8.1	Heller (1980)
7	Bergell	Oligocene	22 samples	331	59	24.1	6.4	Rosenberg and Heller (1997)
6	Lepont. Dom	Oligocene	9 sites	360	63	58.2	6.8	Rosenberg and Heller (1997)
1	Corsica, Sardin.	Karpat/Baden	24 samples	340.6	39.3	58.6	3.9	Speranza et al. (2002)
Apennines								
17	North. Apennines	Torton/Messinian	19 sites	154.6	−51.8	23	7.1	Muttoni et al. (2001)
		E. Oligo.–M. Mioc.	18 site	312.5	42.2	34	6	Muttoni et al. (2001)
	South. Apennines	L.–M. Miocene	2 sites	119	−56	964	8.1	Gattacceca and Speranza (2002)
Eastern Alps								
8	Lower Austria	Karpat/Baden	5 sites	339.2	53.9	86.1	9.4	Scholger and Stingl (2004)
9	Vienna basin	Middle Miocene	4 sites	336.6	57.3	139.1	9	Scholger and Stingl (2004)
20	Klagenfurt basin	L. Sarmatian	6 samples	336	62	44	10	Márton et al. (2000)
21	Lavanttal basin	Pannonian	11 samples	332	61	35	8	Márton et al. (2000)
	Miocene	Ottn.–Karpat	6 sites	293	59	31.6	12.1	Márton et al. (2000)
Intramontane								
	basins	L. Karp.–Pann.	7 sites	328	59	98.3	6.1	Márton et al. (2000)
28	Graz Paleozoic	Miocene	28 samples	47.6	61.4	25.6	5.5	Burgschwaiger et al. (1996)

Locality no. refers to numbers in Fig. 10; Age of ChRM = Age of the characteristic remanent magnetization according to quoted literature; Dec/Inc of ChRM = declination/inclination of the characteristic remanent magnetization according to quoted literature; *K* = precision parameter; á$_{95}$ = radius of cone of 95% confidence about the mean direction (Fisher, 1953).

and Chabert-Pelline, 1999). Obviously, the Northern Calcareous Alps, Central Alps, Southern Alps and their foreland and part of the Western Alps were rotated together.

The rotated unit roughly corresponds to the intra-Alpine part of the Adriatic plate and the units, which were accreted to it during Alpine orogeny up to the Middle Miocene. The northern margin of the rotated block should, therefore, be the surface trace of the basal thrust of the Alpine orogen, and rotation should have taken place on top of the thrust plane. As the youngest deformed sediments at the Alpine front are Middle Miocene in age (Steininger et al., 1991), thrusting and rotation should have terminated during the Late Miocene.

Therefore, present-day structures should in some way reflect eastward increasing thrust distances at the Alpine front due to counter-clockwise rotation. In the Late Oligocene, Helvetic units, which did underlie the foreland basin prior to thrusting, were incorporated into the Alpine nappe stack, and during the Early Miocene, parts of the Oligocene–Miocene fill of the foreland basin were

accreted to the Alpine wedge (Fuchs, 1976; Kempf et al., 1999). In the Swiss Alps and the western sectors of the Eastern Alps, the Helvetic nappes are a thick pile of nappes. Further east, the Helvetic nappes are a thin, discontinuous layer of rock probably boudinaged during nappe transport. Accordingly, the Molasse duplex and triangle zone at the Alpine front have a simple internal structure in the Swiss part of the foreland basin and north of the westernmost Eastern Alps (Vollmayer and Jäger, 1995; Pfiffner et al., 1997), but a rather complex internal structure in the Austrian part of the foreland basin (Wagner et al., 1986). There, the main body of the Alpine orogen completely overthrust the Molasse duplex, and the Flysch and Helvetic units are in direct contact to the autochthonous Molasse.

5.3.2. Counter-clockwise rotation in Late Miocene to Pliocene

A second step of 20° counter-clockwise rotation affected sediments younger than Karpatian in the easternmost part of the Eastern Alps, namely the Klagenfurt and Lavantal basins (Márton et al., 2000), Slovenia/Mura zala (Marton et al., 2002a), northern Croatia (Marton et al., 2002b) and the Styrian and Vienna basins (Scholger and Stingl, 2002) during Pliocene to Quaternary times (Fig. 10).

5.3.3. Reasons for counter-clockwise rotation

The driving force of both counter-clockwise rotations in the Alps might be the rotation of the allochthonous (Apennines) and autochthonous parts of the Adriatic plate, which is a matter of debate in the Cenozoic due to a lack of paleomagnetic data from young sediments, except from the northern part of the Adriatic plate, where paleomagnetic data from Late Eocene to Lower Miocene sedimentary rocks indicate counter-clockwise rotations of about 30° (Thio, 1988; Vandenberg, 1979; Bormioli and Lanza, 1995; Márton et al., 2003c). Counter-clockwise rotation of the Adriatic plate was also proposed on the base of structural data (Vialon et al., 1989; Schmid and Kissling, 2000) and was detected by GPS measurements (Noquet and Calais, 2003).

A striking similarity of paleomagnetic data from the northern Apennines (Muttoni et al., 2001) with the history of counter-clockwise rotation in the Alps can be stated. There, a total of 52° of counter-clockwise rotation was observed in Lower Oligocene sediments, whereas Late Miocene/Pliocene sediments are rotated only by 28°. Rotations in the Eastern Alps are contemporaneous, but do not have the same magnitude. This similarity suggests, that the opening of the Balearic and the Tyrrhenian basins in the Central Mediterranean were not only an effect of retreating subduction of the Adriatic slab below the Apennines (e.g. Bois, 1993; Gueguen et al., 1998), but (also) of a counter-clockwise rotation of the Adriatic plate, probably due to E-directed mantle convection (Doglioni et al., 2002).

6. Conclusion and open questions

The paleomagnetic data presented constrain two main rotation events:

1) A 60° clockwise rotation of the Northern Calcareous Alps between earliest to Late Rupelian. A possible model is clockwise rotation of the Northern Calcareous Alps in a dextral shear corridor between the basal Alpine thrust and the counter-clockwise rotating Central and Southern Alp, which in turn are moving with the Adriatic plate.
2) A 30° counter-clockwise rotation between Late Oligocene and Middle Miocene affected the Eastern Alps, Southern Alps and the internal parts of the Western Alps, as the basal Alpine thrust at this time was below the Middle Penninic units of the Western Alps. Rotation was driven by a counter-clockwise rotation of the Apennines during opening of the Balearic basin.

Both stages of rotations took place during Cenozoic Alpine nappe stacking. In both cases, the allochthonous units of the Alpine nappe stack rotated during translation on the basal thrust. Movement of the nappes was, therefore, by no means dip-slip. Future models of nappe stacking in the Eastern Alps should account for the rotational component of thrusting, which would result in changing thrust distances along strike of nappe boundaries. The most controversial part of this study is the nature and extent of Lower Oligocene clockwise rotation. More data are needed to define the exact boundaries of the block rotated, which will also help to find a well constrained mechanism for clockwise rotation.

Acknowledgments

This study was financed by the Austrian Research Funds (FWF) project: P13566-TEC. For Zijderveld analyses we used the PALDIR software of the Paleomagnetic Laboratory Fort Hoofdijk at the University of Utrecht (NL). The content of the paper was improved by an anonymous reviewer and by the comments by E. Márton, R. Nicolich and the guest editor F. Neubauer. We thank V. Mair for helping us during field work in the Central Alps. S. Hemetsberger was a very helpful,

collegial expert concerning software problems. All this is gratefully acknowledged.

References

Allerton, S., 1998. Geometry and kinematics of vertical-axis rotations in fold and thrust belts. Tectonophysics 199, 15–30.

Aubourg, C., Chabert-Pelline, C., 1999. Neogene remagnetization of normal polarity in the Late Jurassic black shales from the Subalpine chains (French Alps): evidence for late anticlockwise rotations. Tectonophysics 308, 473–486.

Besse, J., Courtillot, V., 2002. Apparent and true polar wander and the geometry of the geomagnetic field over the last 200, Myr. J. Geophys. Res. 107 (B11), 6-1–6–31.

Bois, C., 1993. Initiation and evolution of the Oligo-Miocene rift basins of southwestern Europe: contribution of deep seismic reflection profiling. Tectonophysics 226, 227–252.

Bormioli, D., Lanza, R., 1995. Rotazioni antiorarie nelle rocce terziarie delle Alpi Occidentali e dell'Apennino Settentrionale. In: Polino, R., Sacchi, R. (Eds.), Rapporti Alpi-Appenninio, Scr. Doc. XIV, Roma, pp. 277–289.

Burgschwaiger, E., Mauritsch, H.J., Bierbaumer, M., Scholger, R., 1996. Miocene overprint in the Paleozoic of Graz, Eastern Alps, Austria. Geol. Carpath. 47, 5–12.

Channell, J.E.T., Brandner, R., Spieler, A., Smathers, N.P., 1990. Mesozoic paleogeography of the Northern Calcareous Alps—evidence from paleomagnetism and facies analysis. Geology 18, 828–831.

Channell, J.E.T., Brandner, R., Spieler, A., Stoner, J.S., 1992. Paleomagnetism and paleogeography of the Northern Calcareous Alps (Austria). Tectonics 11, 792–810.

Collinson, D.W., 1983. Methods in Rock Magnetism. Techniques and Instrumentation. Chapman and Hall, London. 503 pp.

Collombet, M., Thomas, J.C., Chauvin, A., Tricart, P., Bouillin, J.P., Gratier, J.P., 2002. Counterclockwise rotation of the western Alps since the Oligocene, new insights from paleomagnetic data. Tectonics 21, 14-1–14–15.

Crouzet, C., Ménard, G., Rochette, P., 1996. Post-Middle Miocene rotations recorded in the Bourg d'Oisans area (Western Alps France) by paleomagnetism. Tectonophysics 263, 137–148.

Dal Piaz, G.V., Del Moro, A., Martin, S., Venturelli, S., 1988. Post-collisional magmatism in the Ortler–Cevedale Massiv, Northern Italy. Jahrb. Geol. Bundesanst. 131, 533–551.

Doglioni, C., Agostini, S., Crespi, M., Innocenti, F., Manetti, P., Riguzzi, F., Savascin, Y., 2002. On the extension in western Anatolia and the Aegean sea. India–Asia convergence in NW Himalaya. In: Rosenbaum, G., Lister, G.S. (Eds.), Reconstruction of the Evolution of the Alpine–Himalayan Orogen, J. Virtual Explorer, vol. 8, pp. 169–183.

Faupl, P., Tollmann, A., 1979. Die Roβfeldschichten, Ein Beispiel für Sedimentation im Bereich einer tektonisch aktiven Tiefseerinne aus der kalkalpinen Unterkreide. Geol. Rundsch. 68 (1), 93–120.

Fisher, R., 1953. Dispersion on a sphere. Proc. R. Soc. London, Ser. A 217, 295–305.

Froitzheim, N., Schmid, S.M., Conti, P., 1994. Repeated change from crustal shortening to orogen-parallel extension in the Austroalpine units of Graubünden. Eclogae Geol. Helv. 87, 559–612.

Froitzheim, N., Schmid, S.M., Frey, M., 1996. Mesozoic paleogeography and the timing of eclogite-facies metamorphism in the Alps, a working hypothesis. Eclogae Geol. Helv. 89/1, 81–110.

Fuchs, W., 1976. Gedanken zur Tektogenese der nördlichen Molasse zwischen Rhone und March. Jahrb. Geol. Bundesanst. 119, 207–249.

Gattacceca, J., Speranza, F., 2002. Paleomagnetism of Jurassic to Miocene sediments from the Apenninic carbonate platform (southern Apennines, Italy): evidence for a 60° counterclockwise Miocene rotation. Earth Planet. Sci. Lett. 201, 19–34.

Gruber, A., 1997. Stratigraphische und strukturelle Analyse im Raum Eiberg (Nördliche Kalkalpen, Unterinntal, Tirol) unter besonderer Berücksichtigung der Entwicklung in der Oberkreide und im Tertiär. Geol. Paläont. Mitt. Innsbruck 22, 159–197.

Gueguen, E., Doglioni, C., Fernandez, M., 1998. On the post-25 Ma geodynamic evolution of the western Mediterranean. Tectonophysics 298, 259–269.

Hagn, H., 1982. Neue Beobachtungen in der Unterkreide der Nördlichen Kalkalpen (Thierseer Mulde etc.). Mitt. Bayer. Staatslg. Paläont. Hist. Geol. 22, 117–135.

Hargraves, R.B., Fisher, A.G., 1959. Remanent magnetism in Jurassic red limestones and radiolarites from the Alps. Geophys. J. 2, 34–41.

Heller, F., 1980. Paleomagnetic evidence for the late Alpine rotation of the Lepontine Area. Eclogae Geol. Helv. 73, 607–618.

Hong Kie, T., 1988. Magnetotectonics in the Piemont Tertiary basin. Phys. Earth Planet Inter. 52, 308–319.

Jung, W., Schleich, H., Kästle, B., 1978. Eine neue stratigraphisch gesicherte Fundstelle für Angiospermen-Früchte und Samen in der oberen Gosau Tirols. Mitt. Bayer. Staatslg. Paläont. Hist. Geol. 18, 131142.

Kappler, P., Zeeh, S., 2000. Relationship between fluid flow and faulting in the Alpine realm (Austria, Germany, Italy). Sediment. Geol. 131, 147–162.

Kempf, O., Matter, A., Burbank, D.W., Mange, M., 1999. Depositional and structural evolution of a foreland basin margin in a magnetostratigraphic framework, the eastern Swiss Molasse Basin. Int. J. Earth Sci. (Geol. Rundsch.) 88, 253–275.

Kirschvink, J.L., 1980. The least squares line and plane and the analysis of paleomagnetic data. Geophys. J. R. Astron. Soc. 62, 699–718.

Krois, P., Stingl, V., Purtscheller, F., 1990. Metamorphosed weathering horizon from the Oetztal–Stubai crystalline complex (Eastern Alps, Austria). Geology 18, 1095–1098.

Lammerer, B., 1986. Das Autochthon im westlichen Tauernfenster. Jahrb. Geol. Bundesanst. 129, 51–67.

Lammerer, B., Weger, M., 1998. Footwall uplift in an orogenic wedge, the Tauern Window in the Eastern Alps of Europe. Tectonophysics 285, 213–230.

Lanza, R., 1977. Paleomagnetic data from the andesitic and lamprophyric dikes of the Sesia–Lanzo zone (Western Alps). Schweiz. Mineral. Petrogr. Mitt. 57, 281–290.

Lanza, R., 1978. Paleomagnetic data on the andesitic cover of the Sesia–Lanzo (Western Alps). Geol. Rundsch. 68, 83–92.

Linzer, H.G., Ratschbacher, L., Frisch, W., 1995. Transpressional collision structures in the upper crust, the fold thrust belt of the Northern Calcareous Alps. Tectonophysics 242, 41–61.

Lowrie, W., 1990. Identification of ferromagnetic minerals by coercivity and unblocking temperatures properties. Geophys. Res. Lett. 17, 159–162.

Maher, B.A., Thompson, R. (Eds.), 1999. Quaternary Climates, Environments, and Magnetism. Cambridge University Press, Cambridge, UK.

Mair, V., Purtscheller, F., 1995. A study on a dyke swarm related to the Königsspitze (Gran Zebru) pluton, Ortler–Campo-crystal-

line (Venosta Valley, W South Tyrol), implications on magma evolution and alteration processes. Geol. Pal. Mitt.Innsbruck 20, 67–86.

Marton, E., Veljovic, D., 1983. Paleomagnetism of the Istria peninsula, Yugoslavia. Tectonophysics 91, 73–87.

Márton, E., Nardi, G., 1994. Cretaceous paleomagnetic data from Murge (Apulia, Southern Italy), tectonic implications. Geophys. J. Int. 119, 842–856.

Márton, E., Kuhlemann, J., Frisch, W., Dunkl, I., 2000. Miocene rotations in the Eastern Alps — palaeomagnetic results from intramontane basin sediments. Tectonophysics 323, 163–182.

Marton, E., Fodor, L., Jelen, B., Marton, P., Rifelj, H., Kevric, R., 2002a. Miocene to Quarternary deformation in NE Slovenia, complex paleomagnetic and structural study. J. Geodyn. 34, 627–651.

Marton, E., Pavelic, D., Tomljenovic, B., Avanic, R., Pamic, J., Marton, P., 2002b. In the wake of a counterclockwise rotating Adriatic microplate, Neogene paleomagnetic results from northern Croatia. Int. J. Earth Sci. 91, 514–523.

Márton, E., Scholger, R., Mauritsch, H.J., Tokarski, A.K., Thöny, W., Krejci, O., 2003a. Counterclockwise rotated Miocene Molasse at the southern margin of stable Europe indicated by paleomagnetic data. In: Csontos, L. (Ed.), 6th Workshop of Alpine Geological Studies, Sopron, Abstracts, Ann. Univ. Sci. Budapest., Sect. Geol., vol. 35, pp. 96–97.

Márton, E., Zampieri, D., Dunkl, I., Frisch, W., Kazmér, M., Braga, G., Grandesso, P., 2003b. Tertiary rotations of the Venetian Alps and their foreland—tectonic implications of new paleomagnetic data. In: Csontos, L. (Ed.), 6th Workshop of Alpine Geological Studies, Sopron, Abstracts, Ann. Univ. Sci. Budapest., Sect. Geol., vol. 35, p. 120.

Márton, E., Drobne, K., Cosovic, V., Moro, A., 2003c. Paleomagnetic evidence for Tertiary counterclockwise rotation of Adria. Tectonophysics 377, 143–156.

Mauritsch, H.J., Becke, M., 1987. Paleomagnetic investigations in the eastern Alps and the Southern Border Zone. In: Flügel, H.W., Faupl, P. (Eds.), Geodynamics of the Eastern Alps. Deuticke, Vienna, pp. 283–308.

McElhinny, M.W., 1964. Statistical significance of the fold test in paleomagnetism. Geophys. J. R. Astron. Soc. 8, 338–340.

Muttoni, G., Lanci, L., Argnani, A., Hirt, A.M., Cibin, U., Abrahamsen, N., Lowrie, W., 2001. Paleomagntic evidence for a Neogene two-phase counterclockwise tectonic rotation in the northern Apennines (Italy). Earth Planet. Sci. Lett. 192, 159–174.

Neubauer, F., 1994. Kontinentkollision in den Ostalpen. Geowissenschaften 12, 136–140.

Noquet, J.M., Calais, E., 2003. Crustal velocity field of western Europe from permanent GPS array solutions. Geophys. J. Int. 154, 72–88.

Ortner, H., 2001. Growing folds and sedimentation of the Gosau Group, Muttekopf, Northern Calcareous Alps, Austria. Int. J. Earth Sci. (Geol. Rundsch.) 90, 727–739.

Ortner, H., 2003. Cementation and tectonics in the Inneralpine Molasse of the Lower Inn Valley. Geol. Paläont. Mitt. Innsbruck 26, 71–89.

Ortner, H., Stingl, V., 2001. Facies and basin development of the Oligocene in the Lower Inn Valley, Tyrol/Bavaria. In: Piller, W., Rasser, M. (Eds.), Paleogene in Austria, Schriftenreihe der Erdwissenschaftlichen Kommissionen, vol. 14, pp. 153–196.

Ortner, H., Reiter, F., Acs, P., 2002. Easy handling of tectonic data, the programs TectonicVB for Mac and TectonicsFP for Windows. Comput. Geosci. 28, 1193–1200.

Pfiffner, O.A., Erard, P.F., Stäuble, M., 1997. Two cross sections through the Swiss Molasse basin (line E4-E6, W1, W7-W10). In: Pfiffner, O.A., Lehner, P., Heitzmann, P., Mueller, S., Steck, A. (Eds.), Results of NRP20. Birkhäuser, Basel, pp. 64--72.

Peacock, D.C.P., Anderson, M.W., Morris, A., Randall, D.E., 1998. Evidence for the importance of "small" faults on block rotation. Tectonophysics 299, 1–13.

Pueyo, E.L., Mauritsch, H.J., Gawlick, H.J., Scholger, R., Frisch, W., 2002. Block, thrust and escape-related rotations in the Central Northern Calcareous Alps. In: Institut Für Geologie Und Paläontologie, Univ. Salzburg (Ed.), Kurzfassungen, PANGEO, Austria., Salzburg, p. 138.

Ratschbacher, L., Frisch, W., Linzer, G., Merle, O., 1991. Lateral extrusion in the Eastern Alps: Part 2. Structural analysis. Tectonics 10, 257–271.

Risch, H., 1985. Gosau.-In: Wolff, H. (Hrsg.), Erläuterungen zum Blatt Bayrischzell, Geologische Karte von Bayern 1:25 000. München, p. 94–99.

Rosenberg, C., Heller, F., 1997. Tilting of the Bergell pluton and Lepontine area, combined evidence from paleomagnetic, structural and petrological data. Eclogae Geol. Helv. 90, 345–356.

Sanders, D., 1998. Tectonically controlled Late Cretaceous terrestrial to neritic deposition (Northern Calcareous Alps, Tyrol, Austria). Facies 39, 139–178.

Schätz, M., Tait, J., Bachtadse, V., Heinisch, H., Soffel, H., 2002. Palaeozoic geography of the Alpine realm, new palaeomagnetic data from the Northern Greywacke Zone, Eastern Alps. Int. J. Earth Sci. (Geol. Rundsch.) 91, 979–992.

Schmid, S.M., Kissling, E., 2000. The arc of the western Alps in the light of geophysical data on deep crustal structure. Tectonics 19, 62–85.

Scholger, R., Stingl, K., 2002. Paleomagnetic reconstruction of geodynamic events in the Eastern Alpine Miocene. In: Institut Für Geologie Und Paläontologie, Univ. Salzburg (Ed.), Kurzfassungen, PANGEO Austria I, Salzburg, pp. 159–160.

Scholger, R., Stingl, K., 2004. New paleomagnetic results from the Middle Miocene (Karpatian and Badenian) in Northern Austria. Geol. Carpath. 55, 199–206.

Speranza, F., Villa, I.M., Sagnotti, L., Florindo, F., Cosentino, D., Cipollari, P., Mattei, M., 2002. Age of the Corsica–Sardinia rotation and Liguro–Provencal basin spreading: new paleomagnetic and Ar/Ar evidence. Tectonophysics 347, 231–251.

Steininger, F.F., Wessely, G., Rögl, F., Wagner, L., 1991. Tertiary sedimentary history and tectonic evolution of the eastern Alpine Foredeep. Giorn. Geol. 48, 285–295.

Stingl, V., Krois, P., 1990. Sedimentological investigations of metamorphic clastics, the basal clastic rocks of the Brenner Mesozoic (Stubai Alps, Austria/Italy). Terra Nova 2, 273–281.

Suk, D., Van Der Voo, R., Peacor, D.R., 1993. Origin of magnetite responsible for remagnetization of Early Paleozoic limestones of New York state. J. Geophys. Res. 98 (B1), 419–434.

Tarling, F., Hrouda, D.H., 1993. The Magnetic Anisotropy of Rocks. Chapman and Hall, London. 217 pp.

Thio, H.K., 1988. Magnetotectonics in the Piemont Tertiary Basin. Phys. Earth Planet. Int. 52, 308–319.

Thiele, O., 1976. Der Nordrand des Tauernfensters zwischen Mayrhofen und Innerschmirn (Tirol). Geol. Rundsch. 65, 410–421.

Thomas, J.C., Claudel, M.E., Collombet, M., Tricart, P., Chauvin, A., Dumont, T., 1999. First paleomagnetic data from the sedimentary cover of the French Penninic Alps, evidence for Tertiary counterclockwise rotations in the Western Alps. Earth Planet. Sci. Lett. 171, 561–574.

Thöni, M., Jagoutz, E., 1993. Isotopic constraints for eo-Alpine high-P metamorphism in the Austroalpine nappes of the Eastern Alps, Its bearing on Alpine orogenesis. Schweiz. Mineral. Petrogr. Mitt. 73, 177–189.

Torsvik, T.H., Briden, J.C., Smethurst, M.A., 1996. SuperIAPD. www.geodynamics.no/iapd/.

TRANSALP Working Group: Gebrande, H., Lüschen, E., Bopp, M., Bleibinhaus, F., Lammerer B., Oncken, O., Stiller, M., Kummerow, J., Kind, R., Millahn, K., Grassl, H., Neubauer, F., Bertelli, L., Borrini, D., Fantoni, R., Pessina, C., Sella, M., Castellarin, A., Nicolich, R., Mazzotti, A., Bernabini, M., 2002. First deep seismic reflection images of the Eastern Alps reveal giant crustal wedges and transcrustal ramps. Geophys. Res. Lett. 29/10, 92-1–92-4.

Urbanek, Ch., Frank, W., Decker, K., 2001. Dating transpressional deformation along the Salzachtal fault (Austria), new implications for the exhumation history of the Tauern window. Abstracts 5th Workshop for Alpine Geological Studies. Geol. Paläont. Mitt. Innsbruck 25, 227–229.

Vandenberg, J., 1979. Preliminary results of a paleomagnetic research on Eocene to Miocene rocks of the Piemont basin (NW Apennines, Italy). Geol. Ultraiectina 20, 147–153.

Vandenberg, J., 1983. Reappraisal of paleomagnetic data from Gargano (south Italy). Tectonophysics 98, 29–41.

Vialon, P., Rochette, P., Menard, G., 1989. Indentation and rotation in the Western Alpine Arc. In: Coward, M.P., Dietrich, D., Park, R.G. (Eds.), Alpine Tectonics, Spec. Publ. Geol. Soc. London, vol. 45, pp. 329–338.

Vollmayer, T., Jäger, S., 1995. Interpretation seismischer Daten und Modell zur Vorbereitung und Auswertung der Bohrung Hindelang 1 (Allgäuer Alpen). Geol. Bav. 100, 153–165.

Wagner, L., Kuckelkorn, K., Hiltmann, W., 1986. Neue Ergebnisse zur alpinen Gebirgsbildung Oberösterreichs aus der Bohrung Oberhofen 1- Stratigraphie, Fazies, Maturität und Tektonik. Erdöl Erdgas Kohle 102/1, 12–19.

Zeeh, St., Walter, U., Kuhlemann, J., Herlec, U., Keppens, E., Bechstedt, Th., 1997. Carbonate cements as tool for fluid flow reconstruction, a study in parts of the Eastern Alps (Austria, Germany, Slovenia). In: Montanez, I.P., Gregg, S.M., Shelton, K.L. (Eds.), Basin-wide diagenetic patterns, Integrated petrologic, geochemical and hydrological considerations, SEPM Special Publication, vol. 57, pp. 167–181.

Zijderveld, J.D.A., 1967. Demagnetization of rocks, Analysis of results. In: Collinson, D.W., Creer, K.M., Runcorn, S.K. (Eds.), Methods in Paleomagnetism. Elsevier, Amsterdam, pp. 254–286.